

**On vanishing gains in robust adaptation of switched systems
A new leakage-based result for a class of Euler–Lagrange dynamics**

Roy, Spandan; Kosmatopoulos, Elias B.; Baldi, Simone

DOI

[10.1016/j.sysconle.2020.104773](https://doi.org/10.1016/j.sysconle.2020.104773)

Publication date

2020

Document Version

Accepted author manuscript

Published in

Systems and Control Letters

Citation (APA)

Roy, S., Kosmatopoulos, E. B., & Baldi, S. (2020). On vanishing gains in robust adaptation of switched systems: A new leakage-based result for a class of Euler–Lagrange dynamics. *Systems and Control Letters*, 144, Article 104773. <https://doi.org/10.1016/j.sysconle.2020.104773>

Important note

To cite this publication, please use the final published version (if applicable).
Please check the document version above.

Copyright

Other than for strictly personal use, it is not permitted to download, forward or distribute the text or part of it, without the consent of the author(s) and/or copyright holder(s), unless the work is under an open content license such as Creative Commons.

Takedown policy

Please contact us and provide details if you believe this document breaches copyrights.
We will remove access to the work immediately and investigate your claim.

On Vanishing Gains in Robust Adaptation of Switched Systems: A New Leakage-based Result for a Class of Euler Lagrange Dynamics

Spandan Roy^{a,b}, Elias B. Kosmatopoulos^d, Simone Baldi^{c,b,*}

^aRobotics Research Center, International Institute of Information Technology Hyderabad, Hyderabad, India

^bDelft Center for Systems and Control (DCSC), Technische Universiteit Delft (TU Delft), Delft, The Netherlands

^cSchool of Mathematics, Southeast University, Nanjing, China

^dDepartment of Electrical and Computer Engineering, Democritus University of Thrace, Xanthi, Greece and Information Technologies Institute, Centre of Research & Technology - Hellas (ITI-CERTH), Thessaloniki, Greece

Abstract

In the presence of unmodelled dynamics and uncertainties with no a priori constant bounds, conventional robust adaptation strategies for switched systems cannot allow the control gains of inactive subsystems to remain constant during inactive intervals: vanishing gains are typically required in order to prove bounded stability. As a consequence, these strategies, known in literature as leakage-based adaptive methods, might introduce poor transients at each switching instant. Leakage-based adaptive control becomes even more problematic in the switched nonlinear case, where non-conservative state-dependent upper bounds for uncertainties and unmodelled dynamics are required. This work shows that, for a class of switched Euler-Lagrange systems, such difficulties can be mitigated: a novel leakage-based stable mechanism is introduced which allows the gains of inactive subsystems to remain constant. At the same time, unmodelled dynamics and uncertainties with no a priori bounds can be handled by a quadratic state-dependent upper bound structure that reduces conservativeness as compared to state-of-the-art structures. The proposed design is validated analytically and its performance is studied in simulation with a pick-and-place robotic manipulator example.

Keywords: Robust adaptive control, Euler-Lagrange systems, Switched systems, Vanishing inactive gains

1. Introduction

Switched systems represent an important class of hybrid systems consisting of subsystems with continuous dynamics and a switching law to regulate the switching among subsystems. The switching can be state-dependent or time-driven, being dwell-time (DT) or average dwell-time (ADT) the most studied classes of time-driven switching [1, 2]. Over the last decade, several works have been reported for control

*Corresponding author

Email addresses: spandan.roy@iiit.ac.in (Spandan Roy), kosmatop@iti.gr (Elias B. Kosmatopoulos), s.baldi@tudelft.nl (Simone Baldi)

¹The research leading to these results has been partially funded by the European Commission H2020-SEC-2016-2017-1, Border Security: autonomous control systems, under contract #740593 (ROBORDER) and H2020-ICT-2014-1, FIRE+ (Future Internet Research & Experimentation), under contract #645220 (RAWFIE), by the Fundamental Research Funds for the Central Universities under contract #4007019109 (RECON-STRUCT), and by the special guiding fund for double first-class under contract #4007019201.

16 of linear [3–6] and nonlinear [7–13] switched systems (see also references therein). Here, we focus specif-
17 ically on *adaptive control of uncertain switched systems*, i.e. control of switched systems with possibly
18 large parametric uncertainties. Recent advances in the field include [14–17] for switched linear systems and
19 [18–24] for classes of switched nonlinear systems.

20 1.1. The issue of robust adaptation and inactive gains

21 In the presence of unmodelled dynamics and uncertainties *with no a priori constant bounds*, it is well
22 known that leakage-based adaptive control is the only robust adaptive mechanism able to prove bounded
23 stability [25, Chap. 8], since projection, switching σ -modification, dead-zone and dynamic normalization
24 all require knowledge of the bounds of the unmodelled dynamics/uncertainties. Efforts have been made
25 recently to design leakage-based adaptive methods for uncertain switched systems. However, it was re-
26 cently demonstrated that switched leakage-based strategies face serious drawbacks as compared to their
27 non-switched counterpart [26–28]. Most notably, [26] showed that the control gains of the inactive sub-
28 systems should decrease exponentially as a consequence of leakage, otherwise bounded stability cannot be
29 proven. This will create poor transients whenever a subsystem that remained inactive for sufficiently long
30 time is activated again. One would desire a situation in which the inactive gains are kept fixed during in-
31 active intervals. Unfortunately, this was shown to be possible only in restrictive cases, such as the class of
32 globally Lipschitz nonlinear dynamics in [28].

33 1.2. The issue of upper bounding uncertainty

34 Leakage-based adaptive control becomes even more challenging for switched nonlinear systems, where
35 the presence of unmodelled dynamics and uncertainties with no a priori constant bounds requires suitable
36 (possibly non-conservative) state-dependent upper bound structures. It is worth mentioning that conserva-
37 tive upper bound structures typically require high inputs, e.g. achieved by monotonically increasing control
38 gains [19, 20, 28]. This work focuses on how conservative structures arise for the class of switched Euler-
39 Lagrange (EL) systems, relevant in many application domains and recurring motif in adaptive switched
40 literature. For example, the switched linear uncertain systems considered in [14, 15, 17, 26] (aircraft, elec-
41 tromechanical systems etc.) are linearized switched dynamics that should be more appropriately described
42 as switched EL dynamics. Even the state-space linear-in-the-parameter (LIP) dynamics in [18, 22–24] can
43 cover only a small class of EL dynamics, since the state-space EL form is in general nonlinear-in-the-
44 parameter (NLIP) due to the inversion of the mass matrix. Even the NLIP structures in [19, 20] might be
45 conservative for EL systems: while being extremely useful to attain strong stability results, the EL examples
46 in [19, 20] reveal that such structures, relying on the parameter separation method pioneered in [29], require
47 detailed structural knowledge of the system dynamics and result in a state-dependent quartic polynomial
48 upper bound to the uncertainties. But it is known that, under mild assumptions [30], uncertainties in EL
49 dynamics can be upper bounded by a less conservative state-dependent quadratic polynomial.

50 1.3. Main contributions

51 In light of the above discussions, leakage-based adaptive switched control presents unsolved challenges.
52 This work proposes a new adaptation method in this direction with the following contributions:

- 53 • A novel leakage-based adaptive mechanism is proposed which avoids the undesirable phenomenon
54 of vanishing control gains. This is achieved by introducing auxiliary gains specifically for leakage
55 purpose, which allow the control gains of inactive subsystems to be kept at the same value they had
56 at switch-out instant.

57 • Such leakage-based strategy is embedded in an adaptation framework for switched EL systems where
 58 uncertainties are upper bounded by a less conservative state-dependent quadratic polynomial struc-
 59 ture, requiring less structural knowledge than LIP or parameter separation-based structures proposed
 60 in literature.

61 This work studies the same class of switched dynamics studied by some of the same authors in [31].
 62 In addition to proposing a new leakage-based adaptation law, this work also manages to remove some
 63 structural constraints present in [31]. More specifically, as compared to [31], the switching law and leakage
 64 terms proposed in this work are independent of system dynamics terms, thus freely tunable. The rest of the
 65 paper is organized as follows: Section 2 describes the uncertain switched EL dynamics; Section 3 details the
 66 proposed control framework, with stability analysis carried out in Section 4; a simulation study is provided
 67 in Section 5, while Section 6 presents concluding remarks.

68 The following notations are used throughout the paper: $\lambda_{\min}(\bullet)$, $\lambda_{\max}(\bullet)$ and $\|\bullet\|$ represent minimum
 69 eigenvalue, maximum eigenvalue and Euclidean norm of (\bullet) respectively; \mathbf{I} denotes identity matrix with
 70 appropriate dimension; \mathbb{R}^+ , \mathbb{N}^+ denote the set of positive real numbers and set of positive integers, re-
 71 spectively; $\Omega = [1, 2, \dots, N]$ denotes the set subsystems and $\mathcal{N}(p)$ denotes the set of inactive subsystem
 72 corresponding to an active subsystem $p \in \Omega$.

73 2. System Dynamics and Problem Formulation

74 Consider the following class of switched Euler-Lagrange (EL) systems

$$\mathbf{M}_\sigma(\mathbf{q})\ddot{\mathbf{q}} + \mathbf{C}_\sigma(\mathbf{q}, \dot{\mathbf{q}})\dot{\mathbf{q}} + \mathbf{G}_\sigma(\mathbf{q}) + \mathbf{F}_\sigma(\dot{\mathbf{q}}) + \mathbf{d}_\sigma = \boldsymbol{\tau}_\sigma, \quad (1)$$

75 where $\mathbf{q} \in \mathbb{R}^n$ is the system state and $\sigma(t) : [0, \infty) \mapsto \Omega$ is a piecewise constant function of time, called the
 76 switching signal, taking values in $\Omega = [1, 2, \dots, N]$; for each subsystem σ , $\mathbf{M}_\sigma(\mathbf{q}) \in \mathbb{R}^{n \times n}$ is the mass/inertia
 77 matrix; $\mathbf{C}_\sigma(\mathbf{q}, \dot{\mathbf{q}}) \in \mathbb{R}^{n \times n}$ are Coriolis/centripetal terms; $\mathbf{G}_\sigma(\mathbf{q}) \in \mathbb{R}^n$ denotes the gravity vector; $\mathbf{F}_\sigma(\dot{\mathbf{q}}) \in \mathbb{R}^n$
 78 represents the vector of damping and friction forces; $\mathbf{d}_\sigma(t) \in \mathbb{R}^n$ denotes bounded external disturbance and
 79 $\boldsymbol{\tau}_\sigma \in \mathbb{R}^n$ is the generalized control input. The switching signal σ make the system terms \mathbf{M}_σ , \mathbf{C}_σ , \mathbf{G}_σ , \mathbf{F}_σ
 80 and the signals \mathbf{d}_σ , $\boldsymbol{\tau}_\sigma$ possibly jump: however, notice that the variables $\mathbf{q}, \dot{\mathbf{q}}$ are continuous (i.e. do not
 81 jump) at the switching instants.

82 **Assumption 1.** *Each subsystem in (1) obeys the following two properties, which hold for many EL systems*
 83 *of practical interest [30]:*

84 **Property 1:** $\exists \bar{c}_\sigma, \bar{g}_\sigma, \bar{f}_\sigma, \bar{d}_\sigma \in \mathbb{R}^+$ such that $\|\mathbf{C}_\sigma(\mathbf{q}, \dot{\mathbf{q}})\| \leq \bar{c}_\sigma \|\dot{\mathbf{q}}\|$, $\|\mathbf{G}_\sigma(\mathbf{q})\| \leq \bar{g}_\sigma$, $\|\mathbf{F}_\sigma(\dot{\mathbf{q}})\| \leq \bar{f}_\sigma \|\dot{\mathbf{q}}\|$ and
 85 $\|\mathbf{d}_\sigma(t)\| \leq \bar{d}_\sigma$.

86 **Property 2:** *The matrix $\mathbf{M}_\sigma(\mathbf{q})$ is symmetric and uniformly positive definite for all \mathbf{q} . This implies that*
 87 $\exists \underline{m}_\sigma, \bar{m}_\sigma \in \mathbb{R}^+$ such that

$$0 < \underline{m}_\sigma \mathbf{I} \leq \mathbf{M}_\sigma(\mathbf{q}) \leq \bar{m}_\sigma \mathbf{I}. \quad (2)$$

88 Further, let \mathbf{M}_σ be decomposed as $\mathbf{M}_\sigma \triangleq \hat{\mathbf{M}}_\sigma + \Delta\mathbf{M}_\sigma$, where $\hat{\mathbf{M}}_\sigma$ and $\Delta\mathbf{M}_\sigma$ represent the nominal and
 89 perturbation terms of \mathbf{M}_σ , respectively. The nominal mass matrix is given, while the perturbation term
 90 (or better, its upper bound) is calculated accounting for the uncertainty in the physical parameters. The
 91 control design challenge in terms of available knowledge of EL system (1) stems from the fact that *only*
 92 *the knowledge of $\hat{\mathbf{M}}_\sigma$ and an upper bound for $\Delta\mathbf{M}_\sigma$ are available; the terms $\mathbf{C}_\sigma, \mathbf{F}_\sigma, \mathbf{G}_\sigma$ and \mathbf{d}_σ (and their*
 93 *upper bounds $\bar{c}_\sigma, \bar{f}_\sigma, \bar{g}_\sigma$ and \bar{d}_σ) are completely unknown.* The following assumption defines the allowed
 94 uncertainty around $\hat{\mathbf{M}}_\sigma$:

95 **Assumption 2.** There exist known scalars \bar{E}_σ such that for $\mathbf{E}_\sigma \triangleq (\mathbf{M}_\sigma^{-1}\hat{\mathbf{M}}_\sigma - \mathbf{I})$ the following holds

$$\|\mathbf{E}_\sigma\| \leq \bar{E}_\sigma < 1, \quad \forall \sigma \in \Omega. \quad (3)$$

96 **Remark 1.** Assumption 2 is not proposed here, but extensively used in literature dealing with EL systems
 97 such as inverse dynamics (cf. [30, §11]) and adaptive sliding mode [32, 33] designs. Such literature shows
 98 that the nominal mass matrix $\hat{\mathbf{M}}_\sigma$ can be selected such that (3) is satisfied by making use of Property 2
 99 (cf. [30, §11]). Essentially, \bar{E}_σ depends on the size of uncertainty around the nominal value of the mass
 100 matrix. The larger the uncertainty, the larger \bar{E}_σ (subject to the fact that \bar{E}_σ should be below 1 for stability
 101 analysis).

102 For ease of control design, system (1) is represented as

$$\ddot{\mathbf{q}} = \mathbf{f}_\sigma(\mathbf{q}, \dot{\mathbf{q}}) + \mathbf{M}_\sigma^{-1} \boldsymbol{\tau}_\sigma, \quad \sigma(t) \in \Omega \quad (4)$$

103 where $\mathbf{f}_\sigma \triangleq -\mathbf{M}_\sigma^{-1}(\mathbf{C}_\sigma + \mathbf{F}_\sigma + \mathbf{G}_\sigma + \mathbf{d}_\sigma)$.

104 Let us define $\mathbf{x} \triangleq [\mathbf{q}^T \ \dot{\mathbf{q}}^T]^T$ which we assume to be available as feedback. Using Properties 1 and 2, the
 105 system dynamics term $\mathbf{f}_\sigma(\mathbf{x})$ can be upper bounded as:

$$\|\mathbf{f}_\sigma(\mathbf{x})\| \leq \theta_{0\sigma} + \theta_{1\sigma}\|\mathbf{x}\| + \theta_{2\sigma}\|\mathbf{x}\|^2 \triangleq \mathbf{Y}_\sigma^T(\|\mathbf{x}\|)\boldsymbol{\Theta}_\sigma, \quad (5)$$

106 where $\mathbf{Y}_\sigma(\|\mathbf{x}\|) = [\mathbf{1} \ \|\mathbf{x}\| \ \|\mathbf{x}\|^2]^T$, $\boldsymbol{\Theta}_\sigma = [\theta_{0\sigma} \ \theta_{1\sigma} \ \theta_{2\sigma}]^T$ and $\theta_{i\sigma} \in \mathbb{R}^+$ $i = 0, 1, 2$ are finite but *unknown*
 107 scalars, according to the available knowledge of system (1).

Remark 2. In the presence of unmodelled dynamics and uncertainties with no a priori bounds, the quadratic upper bound (5) finds its rationale in reduction of conservativeness when minimal structural knowledge is available. In fact, the quadratic structure (5) is general, i.e. it holds for many EL systems irrespective of their specific structure [30, 32, 33]. On the other hand, let us consider an alternative upper bound structure proposed in [19, 20]

$$\|\mathbf{f}_\sigma(\mathbf{x})\| \leq \varphi_\sigma(\mathbf{x})\phi_\sigma(\boldsymbol{\theta}_\sigma) \quad (6)$$

108 where $\varphi_\sigma(\mathbf{x}) \geq 1$, $\phi_\sigma(\boldsymbol{\theta}_\sigma) \geq 1$ are two scalar functions and $\boldsymbol{\theta}_\sigma$ denotes the set of unknown system param-
 109 eters. The structure (6) is extremely useful to attain strong (asymptotic) stability results, but there is no
 110 general procedure for deriving appropriate scalar functions in (6). In particular, for EL dynamics (4), deep
 111 structural knowledge of the system is required to derive such scalar functions (cf. the examples in [19, 20]).

112 We use the notation $\{(\sigma(t_l), t_l) \mid l \in \mathbb{N}^+ \cup \{0\}\}$ to denote the set of (subsystem, switching instant) pairs.
 113 The sequence of switch-in and switch-out instants of subsystem p , $p \in \Omega$ is given as $\{t_{p_1}, t_{p_2}, \dots, t_{p_l}, \dots \mid l \in$
 114 $\mathbb{N}^+\}$ and $\{t_{p_{l+1}}, t_{p_{2+1}}, \dots, t_{p_{l+1}}, \dots \mid l \in \mathbb{N}^+\}$, respectively. The following class of switching signals is
 115 considered:

Definition 1. Average Dwell Time (ADT) [2]: For a switching signal $\sigma(t)$ and each $t_2 \geq t_1 \geq 0$, let $N_\sigma(t_1, t_2)$ denote the number of discontinuities in the interval $[t_1, t_2)$. Then $\sigma(t)$ has an average dwell time ϑ if for a given scalar $N_0 > 0$

$$N_\sigma(t_1, t_2) \leq N_0 + (t_2 - t_1)/\vartheta, \quad \forall t_2 \geq t_1 \geq 0$$

116 where N_0 is termed as chatter bound.

117 3. Controller Design

118 Let us consider the tracking problem for a desired trajectory $\mathbf{q}^d(t)$ satisfying the following assumption.

119 **Assumption 3.** *The desired trajectories are smooth enough, in particular $\mathbf{q}^d, \dot{\mathbf{q}}^d, \ddot{\mathbf{q}}^d \in \mathcal{L}_\infty$.*

Let $\mathbf{e}(t) \triangleq \mathbf{q}(t) - \mathbf{q}^d(t)$ be the tracking error and $\xi(t) \triangleq [\mathbf{e}(t), \dot{\mathbf{e}}(t)]$. We define a filtered tracking error variable \mathbf{r}_σ as

$$\mathbf{r}_\sigma \triangleq \mathbf{B}^T \mathbf{P}_\sigma \xi, \quad \sigma \in \Omega \quad (7)$$

120 where $\mathbf{P}_\sigma > \mathbf{0}$ is the solution to the Lyapunov equation $\mathbf{A}_\sigma^T \mathbf{P}_\sigma + \mathbf{P}_\sigma \mathbf{A}_\sigma = -\mathbf{Q}_\sigma$ for some $\mathbf{Q}_\sigma > \mathbf{0}$, $\mathbf{A}_\sigma \triangleq$
 121 $\begin{bmatrix} \mathbf{0} & \mathbf{I} \\ -\mathbf{K}_{1\sigma} & -\mathbf{K}_{2\sigma} \end{bmatrix}$ and $\mathbf{B} \triangleq [\mathbf{0} \ \mathbf{I}]^T$. Here, $\mathbf{K}_{1\sigma}$ and $\mathbf{K}_{2\sigma}$ are two user-defined positive definite gain matrices
 122 and their positive definiteness guarantees \mathbf{A}_σ to be Hurwitz.

The switched control law is designed as

$$\tau_\sigma = \hat{\mathbf{M}}_\sigma (-\Lambda_\sigma \xi - \Delta\tau_\sigma + \ddot{\mathbf{q}}^d), \quad (8a)$$

$$\Delta\tau_\sigma = \omega \rho_\sigma \frac{\mathbf{r}_\sigma}{\sqrt{\|\mathbf{r}_\sigma\|^2 + \varepsilon}}, \quad (8b)$$

where $\Lambda_\sigma \triangleq [\mathbf{K}_{1\sigma} \ \mathbf{K}_{2\sigma}]$; $\Delta\tau_\sigma$ tackles the uncertainties utilizing the gain ρ_σ ; $\varepsilon > 0$ is a small scalar to avoid control chatter and $\omega > 1$ is a user-defined scalar. The design of ρ_σ will be discussed later. Let $\eta_\sigma \triangleq (-\Lambda_\sigma \xi - \Delta\tau_\sigma + \ddot{\mathbf{q}}^d)$. Now, substituting (8a) in (4) yields

$$\begin{aligned} \ddot{\mathbf{e}} &= \ddot{\mathbf{q}} - \ddot{\mathbf{q}}^d \\ &= \mathbf{f}_\sigma + \mathbf{M}_\sigma^{-1} \tau_\sigma - \ddot{\mathbf{q}}^d \\ &= \mathbf{f}_\sigma + (\mathbf{M}_\sigma^{-1} \hat{\mathbf{M}}_\sigma - \mathbf{I}) \eta_\sigma + \eta_\sigma - \ddot{\mathbf{q}}^d \\ &= -\Lambda_\sigma \xi - \Delta\tau_\sigma - \mathbf{E}_\sigma \Delta\tau_\sigma + \Psi_\sigma, \end{aligned} \quad (9)$$

123 where $\Psi_\sigma \triangleq \mathbf{f}_\sigma + \mathbf{E}_\sigma (\ddot{\mathbf{q}}^d - \Lambda_\sigma \xi)$ is treated as the overall uncertainty. Hence, using Assumptions 1 and 2,
 124 one can verify the existence of $\theta_{i\sigma}^* \in \mathbb{R}^+$ $i = 0, 1, 2$ such that for all $\sigma \in \Omega$

$$\|\Psi_\sigma\| \leq \theta_{0\sigma}^* + \theta_{1\sigma}^* \|\xi\| + \theta_{2\sigma}^* \|\xi\|^2 \triangleq \mathbf{Y}_\sigma^T (\|\xi\|) \Theta_\sigma^*, \quad (10)$$

where $\theta_{i\sigma}^*$'s are unknown finite scalars and $\Theta_\sigma^* = [\theta_{0\sigma}^* \ \theta_{1\sigma}^* \ \theta_{2\sigma}^*]^T$. After defining the structures of the upper bound of $\|\Psi_\sigma\|$ in (10), the gain ρ_σ in (8b) is proposed as

$$\rho_\sigma = \frac{1}{1 - \bar{E}_\sigma} \{ (\hat{\theta}_{0\sigma} + \gamma_{0\sigma}) + (\hat{\theta}_{1\sigma} + \gamma_{1\sigma}) \|\xi\| + (\hat{\theta}_{2\sigma} + \gamma_{2\sigma}) \|\xi\|^2 \} \triangleq \frac{1}{1 - \bar{E}_\sigma} \mathbf{Y}_\sigma^T (\|\xi\|) (\hat{\Theta}_\sigma + \Gamma_\sigma), \quad (11)$$

125 where $\hat{\Theta}_\sigma \triangleq [\hat{\theta}_{0\sigma} \ \hat{\theta}_{1\sigma} \ \hat{\theta}_{2\sigma}]^T$ is the estimate of Θ_σ^* ; $\Gamma_\sigma \triangleq [\gamma_{0\sigma} \ \gamma_{1\sigma} \ \gamma_{2\sigma}]^T$ is an auxiliary gain which has a
 126 crucial role in closed-loop system stabilization and it will be detailed later.

Let p denote the index of the subsystem active for $t \in [t_l \ t_{l+1})$ and $\mathcal{N}(p)$ denote the set of inactive subsystems. The gains $\hat{\theta}_{ip}, \gamma_{ip}$ are evaluated using the following laws:

$$\dot{\hat{\theta}}_{ip} = \|\mathbf{r}_p\| \|\xi\|^i - \alpha_{ip} \hat{\theta}_{ip}, \quad \dot{\gamma}_{ip} = 0 \quad (12a)$$

$$\dot{\hat{\theta}}_{i\bar{p}} = 0, \quad \dot{\gamma}_{i\bar{p}} = -(\beta_{i\bar{p}} + \bar{v}_{i\bar{p}} \hat{\theta}_{i\bar{p}}^4) \gamma_{i\bar{p}} + \beta_{i\bar{p}} v_{i\bar{p}}, \quad (12b)$$

$$\text{with } \hat{\theta}_{ip}(t_0) > 0, \gamma_{i\bar{p}}(t_0) > v_{i\bar{p}}, \quad (12c)$$

where $\bar{p} \in \mathcal{N}(p)$; $\alpha_{i\bar{p}}, \beta_{i\bar{p}}, \nu_{i\bar{p}}, \bar{\nu}_{i\bar{p}} \in \mathbb{R}^+$, $i = 0, 1, 2$ are static design scalars and t_0 is the initial time. Investigating the adaptive laws (12a)-(41) and the initial gain conditions (12c), it can be verified that there exists a positive fixed scalar $\underline{\gamma}_{i\bar{p}}$ such that

$$\hat{\theta}_{i\bar{p}}(t) \geq 0 \text{ and } \gamma_{i\bar{p}}(t) \geq \underline{\gamma}_{i\bar{p}} > 0 \quad \forall t \geq t_0. \quad (13)$$

127 The above condition is later exploited during the stability analysis. The following remark illustrates the major
128 differences between (11)-(12) and state-of-the-art robust adaptive laws for uncertain switched systems.

129 **Remark 3.** In [26], bounded stability requires that the gains for the inactive systems (corresponding to $\hat{\theta}_{i\bar{p}}$
130 in our case) vanish exponentially, as an effect of leakage. This implies that, if a system remains inactive for
131 sufficiently long time, its gains drop to zero, generating a new transient at switch-on times. This vanishing-
132 gain scenario is avoided by (41) where the adaptive gains of inactive subsystems are kept at the same
133 value before switch-off time. In [27] bounded stability requires the adaptive laws for all active and inactive
134 subsystem to be constantly active as the tracking error drives all of them simultaneously. A more preferable
135 situation arises in (11)-(12), where only a limited set of the adaptive laws is actively driven by the tracking
136 error.

We define $\zeta_{Mp} \triangleq \lambda_{\max}(\mathbf{P}_p)$, $\zeta_{mp} \triangleq \lambda_{\min}(\mathbf{P}_p)$, $\bar{\zeta}_M \triangleq \max_{p \in \Omega} \zeta_{Mp}$ and $\underline{\zeta}_m \triangleq \min_{p \in \Omega} \zeta_{mp}$. Following Definition 1 of ADT [2], the switching law is proposed as

$$\vartheta > \vartheta^* = \ln \mu / \kappa, \quad (14)$$

137 where $\mu \triangleq \bar{\zeta}_M / \underline{\zeta}_m$; κ is a scalar defined as $0 < \kappa < \zeta$ where $\zeta_p \triangleq (\lambda_{\min}(\mathbf{Q}_p) / \lambda_{\max}(\mathbf{P}_p))$ and $\zeta \triangleq \min_{p \in \Omega} \{\zeta_p\}$.
138 Note that the proposed leakage terms in (12) and switching law in (14) are independent of system parame-
139 ters.

140 4. Stability Analysis of The Proposed Switched Controller

From the definitions of Λ_σ and ξ we have $\Lambda_\sigma \xi = \mathbf{K}_{1\sigma} \mathbf{e} + \mathbf{K}_{2\sigma} \dot{\mathbf{e}}$. Using this relation, the following error dynamics is obtained from (9)

$$\dot{\xi} = \mathbf{A}_\sigma \xi + \mathbf{B}(\Psi_\sigma - \Delta\tau_\sigma - \mathbf{E}_\sigma \Delta\tau_\sigma). \quad (15)$$

141 Before presenting the closed-loop stability result, let us recall the stability concept sought in switched robust
142 adaptive control [26]:

143 **Definition 2** (Uniform Ultimate Boundedness (UUB)). *The switched system (15) under switching signal*
144 *$\sigma(\cdot)$ is uniformly ultimately bounded if there exists a convex and compact set \mathcal{C} such that for every initial*
145 *condition $\xi(t_0) = \xi_0$, there exists a finite time $T(\xi_0)$ such that $\xi(t) \in \mathcal{C}$ for all $t \geq T(\xi_0)$. Further, a*
146 *constant b , independent of initial time t_0 , is said to be the ultimate bound if $\|\xi(t)\| \leq b$ for all $t \geq T(\xi_0)$.*

147 **Theorem 1.** *Under Assumptions 1-3, the closed-loop trajectories of system (4) employing the control laws*
148 *(8) and (11) associated with adaptive law (12) and switching law (14) are UUB if the gains $\alpha_{i\bar{p}}$ and $\beta_{i\bar{p}}$ are*
149 *designed as $\alpha_{i\bar{p}} > \zeta_p/2$ and $\beta_{i\bar{p}} > \zeta_{\bar{p}}/2$.*

Proof. The closed-loop stability analysis follows similar lines as the proof of Theorem 1 of [31], with the difference that the following Lyapunov-like candidate is considered

$$V(\xi(t), \tilde{\theta}_{ip}(t), \gamma_{ip}(t), t) = (1/2)\xi^T(t)\mathbf{P}_{\sigma(t)}\xi(t) + (1/2)\sum_{p=1}^N\sum_{i=0}^2\{(\hat{\theta}_{ip}(t) - \theta_{ip}^*)^2 + \gamma_{ip}^2(t)\}, \quad (16)$$

150 where $\tilde{\theta}_{ip}(t) = (\hat{\theta}_{ip}(t) - \theta_{ip}^*)$. For brevity, we will sometimes express $V(\xi(\cdot), \tilde{\theta}_{ip}(\cdot), \gamma_{ip}(\cdot), \cdot) = V(\cdot)$ to high-
 151 light the time evolution of (16). Note that the function (16) depends explicitly on time, due to the active
 152 subsystem $\sigma(t)$. This implies that (16) is a multiple Lyapunov-like function, popular in switched systems
 153 literature [2]. In fact, \mathbf{P}_p can be designed differently for different subsystems due to the requirements, in-
 154 dicating that $V(\cdot)$ might be discontinuous at the switching instants and only remains continuous during the
 155 time interval of two consecutive switchings. Such a switched framework requires to study the behaviour of
 156 (16) at and in between switching instants, as carried out subsequently.

157
 158 **Analysis of the Lyapunov function at switching instants:** We denote with $\sigma(t_{l+1}^-)$ the active sub-
 159 system when $t \in [t_l, t_{l+1})$ and with $\sigma(t_{l+1})$ the active subsystem when $t \in [t_{l+1}, t_{l+2})$. Then, although the
 160 Lyapunov-like candidate is different, one can still follow similar lines as the proof of Theorem 1 in [31],
 161 obtaining that the following behaviour of $V(\cdot)$ is true at the switching instant t_{l+1} , $l \in \mathbb{N}^+$:

$$\begin{aligned} V(t_{l+1}) - V(t_{l+1}^-) &\leq \frac{\bar{\zeta}_M - \underline{\zeta}_m}{\underline{\zeta}_m} V(t_{l+1}^-) \\ &\Rightarrow V(t_{l+1}) \leq \mu V(t_{l+1}^-), \end{aligned} \quad (17)$$

162 with $\mu = \bar{\zeta}_M / \underline{\zeta}_m \geq 1$ and t_{l+1}^- denotes the time instant right before switching at $t = t_{l+1}$ (i.e. the limit from
 163 the left of t_{l+1}).

164
 165 **Analysis of the Lyapunov function in between switching instants:** This analysis refers to the be-
 166 haviour of $V(\cdot)$ when $t \in (t_l, t_{l+1})$. Note that $V(\cdot)$ is piecewise differentiable, and differentiable for
 167 $t \in (t_l, t_{l+1})$, $l \in \mathbb{N}^+$, so that its time-derivative is well defined.

Using (7), (15) and the Lyapunov equation $\mathbf{A}_{\sigma}^T \mathbf{P}_{\sigma} + \mathbf{P}_{\sigma} \mathbf{A}_{\sigma} = -\mathbf{Q}_{\sigma}$, the time derivative of (16) yields

$$\begin{aligned} \dot{V}(t) &= (1/2)\xi^T(t)(\mathbf{A}_{\sigma(t_{l+1}^-)}^T \mathbf{P}_{\sigma(t_{l+1}^-)} + \mathbf{P}_{\sigma(t_{l+1}^-)} \mathbf{A}_{\sigma(t_{l+1}^-)})\xi(t) + \xi^T(t)\mathbf{P}_{\sigma(t_{l+1}^-)}\mathbf{B}\left(\Psi_{\sigma(t_{l+1}^-)} - (\mathbf{I} + \mathbf{E}_{\sigma(t_{l+1}^-)})\Delta\tau_{\sigma(t_{l+1}^-)}\right) \\ &\quad + \sum_{p=1}^N\sum_{i=0}^2\left\{(\hat{\theta}_{ip}(t) - \theta_{ip}^*)\dot{\hat{\theta}}_{ip}(t) + \gamma_{ip}(t)\dot{\gamma}_{ip}(t)\right\} \\ &= -(1/2)\xi^T(t)\mathbf{Q}_{\sigma(t_{l+1}^-)}\xi(t) + \mathbf{r}_{\sigma(t_{l+1}^-)}^T\left(\Psi_{\sigma(t_{l+1}^-)} - (\mathbf{I} + \mathbf{E}_{\sigma(t_{l+1}^-)})\Delta\tau_{\sigma(t_{l+1}^-)}\right) \\ &\quad + \sum_{p=1}^N\sum_{i=0}^2\left\{(\hat{\theta}_{ip}(t) - \theta_{ip}^*)\dot{\hat{\theta}}_{ip}(t) + \gamma_{ip}(t)\dot{\gamma}_{ip}(t)\right\} \\ &\leq -(1/2)\xi^T(t)\mathbf{Q}_{\sigma(t_{l+1}^-)}\xi(t) + \|\Psi_{\sigma(t_{l+1}^-)}\|\|\mathbf{r}_{\sigma(t_{l+1}^-)}\| - (1 - \bar{E}_{\sigma(t_{l+1}^-)})\rho_{\sigma(t_{l+1}^-)}\frac{\|\mathbf{r}_{\sigma(t_{l+1}^-)}\|^2}{\sqrt{\|\mathbf{r}_{\sigma(t_{l+1}^-)}\|^2 + \varepsilon}} \\ &\quad + \sum_{p=1}^N\sum_{i=0}^2\left\{(\hat{\theta}_{ip}(t) - \theta_{ip}^*)\dot{\hat{\theta}}_{ip}(t) + \gamma_{ip}(t)\dot{\gamma}_{ip}(t)\right\}. \end{aligned} \quad (18)$$

Notice that, here and in the following, the time index t is kept only for $\xi(t)$, $\hat{\theta}_{ip}(t)$, $\gamma(t)$ and otherwise omitted for brevity. For the ease of analysis, we define a region such that

$$\omega \frac{\|\mathbf{r}_\sigma\|^2}{\sqrt{\|\mathbf{r}_\sigma\|^2 + \varepsilon}} \geq \|\mathbf{r}_\sigma\| \Rightarrow \|\mathbf{r}_\sigma\| \geq \sqrt{\frac{\varepsilon}{\omega^2 - 1}} \triangleq \varphi. \quad (19)$$

168 The condition (19) implies that one needs to select $\omega > 1$, which is always possible since ω is a user defined
169 scalar.

170
171 **Establishing exponential decrease of the Lyapunov function:** Up to now we have established (17) at
172 switching instants, and (18) in between switching instants. A crucial mechanism for establishing stability
173 of a switched system is that the possible jump of the Lyapunov function at (17) is compensated by some
174 exponential decrease of the Lyapunov function via (18). Therefore, in the following we will rewrite (18) to
175 highlight the exponential decrease. Subsequently, we proceed with the stability analysis for two scenarios:

176 S1: $\|\mathbf{r}_\sigma\| \geq \varphi$ and

177 S2: $\|\mathbf{r}_\sigma\| < \varphi$.

178 We study the behaviour of the Lyapunov function for these two scenarios as below.

Scenario S1: The adaptive law (12) reveals that the gains $\hat{\theta}_{i\bar{p}}$ and $\gamma_{i\bar{p}}$ remain constant during inactive and active intervals, respectively. Therefore, utilizing these observations and the upper bound structure (10) of uncertainty, (18) is simplified for $t \in (t_l \ t_{l+1})$ as

$$\begin{aligned} \dot{V}(t) \leq & -(1/2)\xi^T(t)\mathbf{Q}_{\sigma(t_{l+1}^-)}\xi(t) - \mathbf{Y}_{\sigma(t_{l+1}^-)}^T(\hat{\Theta}_{\sigma(t_{l+1}^-)} - \Theta_{\sigma(t_{l+1}^-)}^*)\|\mathbf{r}_{\sigma(t_{l+1}^-)}\| \\ & + \sum_{i=0, p=\sigma(t_{l+1}^-)}^2 (\hat{\theta}_{ip}(t) - \theta_{ip}^*)\dot{\hat{\theta}}_{ip}(t) + \sum_{\bar{p} \in \mathcal{N}(p)} \sum_{i=0}^2 \gamma_{i\bar{p}}(t)\dot{\gamma}_{i\bar{p}}(t). \end{aligned} \quad (20)$$

Using (12a) we have for $p = \sigma(t_{l+1}^-)$

$$\begin{aligned} \sum_{i=0}^2 (\hat{\theta}_{ip} - \theta_{ip}^*)\dot{\hat{\theta}}_{ip} &= \sum_{i=0}^2 (\hat{\theta}_{ip} - \theta_{ip}^*)(\|\mathbf{r}_p\| \|\xi\|^i - \alpha_{ip}\hat{\theta}_{ip}) \\ &= \sum_{i=0}^2 \|\mathbf{r}_p\| (\hat{\theta}_{ip} - \theta_{ip}^*) \|\xi\|^i + \alpha_{ip}\hat{\theta}_{ip}\theta_{ip}^* - \alpha_{ip}\hat{\theta}_{ip}^2 \\ &= \mathbf{Y}_p^T(\hat{\Theta}_p - \Theta_p^*)\|\mathbf{r}_p\| + \sum_{i=0}^2 \{\alpha_{ip}\hat{\theta}_{ip}\theta_{ip}^* - \alpha_{ip}\hat{\theta}_{ip}^2\}. \end{aligned} \quad (21)$$

Similarly, (41) leads to

$$\gamma_{i\bar{p}}\dot{\gamma}_{i\bar{p}} = -(\beta_{i\bar{p}} + \bar{\nu}_{i\bar{p}}\hat{\theta}_{i\bar{p}}^4)\gamma_{i\bar{p}}^2 + \beta_{i\bar{p}}\nu_{i\bar{p}}\gamma_{i\bar{p}}. \quad (22)$$

From (13) we have $\gamma_{i\bar{p}} \geq \underline{\gamma}_{i\bar{p}} \ \forall t \geq t_0$. Applying this relation to the second term of (22) yields

$$\gamma_{i\bar{p}}\dot{\gamma}_{i\bar{p}} \leq -\beta_{i\bar{p}}\gamma_{i\bar{p}}^2 - \underline{\gamma}_{i\bar{p}}^2\bar{\nu}_{i\bar{p}}\hat{\theta}_{i\bar{p}}^4 + \beta_{i\bar{p}}\nu_{i\bar{p}}\gamma_{i\bar{p}}. \quad (23)$$

Note that the following equality holds

$$-\underline{\gamma}_{i\bar{p}}^2\bar{\nu}_{i\bar{p}}\hat{\theta}_{i\bar{p}}^4 + (\zeta_{\bar{p}}/2)\hat{\theta}_{i\bar{p}}^2 = -(\underline{\gamma}_{i\bar{p}}\sqrt{\bar{\nu}_{i\bar{p}}}\hat{\theta}_{i\bar{p}}^2 - (\zeta_{\bar{p}}/(4\underline{\gamma}_{i\bar{p}}\sqrt{\bar{\nu}_{i\bar{p}}}))^2) + \zeta_{\bar{p}}^2/(16\underline{\gamma}_{i\bar{p}}\underline{\gamma}_{i\bar{p}}^2). \quad (24)$$

Substituting (21), (23) and (24) in (20) yields for $t \in (t_l \ t_{l+1})$

$$\begin{aligned} \dot{V}(t) \leq & -(1/2)\lambda_{\min}(\mathbf{Q}_{\sigma(t_{l+1}^-)})\|\xi(t)\|^2 + \sum_{i=0}^2 \alpha_{ip} \hat{\theta}_{ip}(t) \theta_{ip}^* - \alpha_{ip} \hat{\theta}_{ip}^2(t) - \left(\sum_{\bar{p} \in \mathcal{N}(p)} \sum_{i=0}^2 \beta_{i\bar{p}} \gamma_{i\bar{p}}^2 + \hat{\theta}_{i\bar{p}}^2 - \beta_{i\bar{p}} \underline{\gamma}_{i\bar{p}} \gamma_{i\bar{p}} \right) \\ & - (1/2)\hat{\theta}_{i\bar{p}}^2 + \zeta_{i\bar{p}}^2 / (16\bar{v}_{i\bar{p}} \underline{\gamma}_{i\bar{p}}^2). \end{aligned} \quad (25)$$

Since $\hat{\theta}_{ip} \geq 0$ by design (13), the definition of Lyapunov function (16) yields

$$V(\xi(t), \tilde{\theta}_{ip}(t), \gamma_{ip}(t), t) \leq \frac{1}{2} \lambda_{\max}(\mathbf{P}_{\sigma}) \|\xi\|^2 + \frac{1}{2} \sum_{p=1}^N \sum_{i=0}^2 (\hat{\theta}_{ip}^2 + \theta_{ip}^{*2} + \gamma_{ip}^2), \quad \forall t. \quad (26)$$

The definitions of ζ , ζ_{Mp} , α_{ip} , $\beta_{i\bar{p}}$ and the use of (26), allows to simplify the condition (25) into

$$\begin{aligned} \dot{V}(t) \leq & -\zeta V(t) + \sum_{i=0, p=\sigma(t_{l+1}^-)}^2 \alpha_{ip} \hat{\theta}_{ip}(t) \theta_{ip}^* - \bar{\alpha}_{ip} \hat{\theta}_{ip}^2(t) + \gamma_{ip}^2(t) + \sum_{p=1}^N \sum_{i=0}^2 \frac{\zeta_p}{2} \theta_{ip}^{*2} \\ & + \sum_{\bar{p} \in \mathcal{N}(p)} \sum_{i=0}^2 \{ \beta_{i\bar{p}} \underline{\gamma}_{i\bar{p}} \gamma_{i\bar{p}}(t) - \bar{\beta}_{i\bar{p}} \gamma_{i\bar{p}}^2(t) + \zeta_{i\bar{p}}^2 / (16\bar{v}_{i\bar{p}} \underline{\gamma}_{i\bar{p}}^2) \}, \quad t \in (t_l \ t_{l+1}) \end{aligned} \quad (27)$$

where $\bar{\alpha}_{ip} \triangleq (\alpha_{ip} - \frac{\zeta_p}{2}) > 0$ and $\bar{\beta}_{i\bar{p}} \triangleq (\beta_{i\bar{p}} - \frac{\zeta_{i\bar{p}}}{2}) > 0$. Note that the following equality holds

$$\alpha_{ip} \hat{\theta}_{ip} \theta_{ip}^* - \bar{\alpha}_{ip} \hat{\theta}_{ip}^2 = -\bar{\alpha}_{ip} \left(\hat{\theta}_{ip} - \frac{\alpha_{ip} \theta_{ip}^*}{2\bar{\alpha}_{ip}} \right)^2 + \frac{(\alpha_{ip} \theta_{ip}^*)^2}{4\bar{\alpha}_{ip}}. \quad (28)$$

The adaptive laws (12) reveals that $\gamma_{i\bar{p}}$ decreases for the inactive systems and remains unchanged for the active system. Together with inequality $\gamma_{ip} \geq \underline{\gamma}_{ip} \quad \forall t \geq t_0$, we obtain that $\gamma_{ip} \in \mathcal{L}_{\infty} \quad \forall p \in \Omega$. Therefore, there exists $\bar{\gamma}_{ip} \in \mathbb{R}^+$ such that $\gamma_{ip}(t) \leq \bar{\gamma}_{ip}$. Using κ such that $0 < \kappa < \zeta$ and using (28), we have that $\dot{V}(t)$ in (27) simplifies to

$$\dot{V}(t) \leq -\kappa V(t) - (\zeta - \kappa)V(t) + \varsigma + \varsigma_2, \quad t \in (t_l \ t_{l+1}) \quad (29)$$

179 with $\varsigma \triangleq \sum_{p=1}^N \sum_{i=0}^2 \frac{\zeta_p}{2} \theta_{ip}^{*2} + \beta_{ip} \underline{\gamma}_{ip} \bar{\gamma}_{ip} + (\zeta_{i\bar{p}}^2 / (16\bar{v}_{i\bar{p}} \underline{\gamma}_{i\bar{p}}^2))$ and $\varsigma_2 \triangleq \sum_{i=0, p=\sigma(t_{l+1}^-)}^2 \frac{(\alpha_{ip} \theta_{ip}^*)^2}{4\bar{\alpha}_{ip}} + \bar{\gamma}_{ip}^2$. Note that
 180 (29) highlights, for Scenario 1, the exponential decrease of the Lyapunov function in a region around the
 181 origin.

Scenario S2: In this scenario we have $\|\mathbf{r}_{\sigma}\| < \varphi$. Therefore, we have for $t \in (t_l \ t_{l+1})$

$$\begin{aligned} \dot{V}(t) \leq & -(1/2)\xi^T(t) \mathbf{Q}_{\sigma(t_{l+1}^-)} \xi(t) - (1 - \bar{E}_{\sigma(t_{l+1}^-)}) \rho_{\sigma(t_{l+1}^-)} \frac{\|\mathbf{r}_{\sigma(t_{l+1}^-)}\|^2}{\sqrt{\|\mathbf{r}_{\sigma(t_{l+1}^-)}\|^2 + \varepsilon}} + \mathbf{Y}_{\sigma(t_{l+1}^-)}^T \Theta_{\sigma(t_{l+1}^-)}^* \|\mathbf{r}_{\sigma(t_{l+1}^-)}\| \\ & + \sum_{i=0, p=\sigma(t_{l+1}^-)}^2 (\hat{\theta}_{ip}(t) - \theta_{ip}^*) \dot{\hat{\theta}}_{ip}(t) + \sum_{\bar{p} \in \mathcal{N}(p)} \sum_{i=0}^2 \gamma_{i\bar{p}}(t) \dot{\gamma}_{i\bar{p}}(t) \\ \leq & -(1/2)\xi^T(t) \mathbf{Q}_{\sigma(t_{l+1}^-)} \xi(t) + \mathbf{Y}_{\sigma(t_{l+1}^-)}^T \Theta_{\sigma(t_{l+1}^-)}^* \|\mathbf{r}_{\sigma(t_{l+1}^-)}\| \\ & + \sum_{i=0, p=\sigma(t_{l+1}^-)}^2 (\hat{\theta}_{ip}(t) - \theta_{ip}^*) \dot{\hat{\theta}}_{ip}(t) + \sum_{\bar{p} \in \mathcal{N}(p)} \sum_{i=0}^2 \gamma_{i\bar{p}}(t) \dot{\gamma}_{i\bar{p}}(t). \end{aligned} \quad (30)$$

Then, following similar lines as in Scenario S1, we have for $t \in (t_l \ t_{l+1})$

$$\dot{V}(t) \leq -\kappa V(t) - (\zeta - \kappa)V(t) + \mathbf{Y}_{\sigma(t_{l+1}^-)}^T \Theta_{\sigma(t_{l+1}^-)}^* \|\mathbf{r}_{\sigma(t_{l+1}^-)}\| + \zeta + \zeta_2. \quad (31)$$

From (7) one can verify $\|\mathbf{r}\| < \varphi \Rightarrow \|\xi\| \in \mathcal{L}_\infty$ and consequently, the adaptive law (12a) implies $\|\mathbf{r}\|, \|\xi\| \in \mathcal{L}_\infty \Rightarrow \hat{\theta}_{ip}(t) \in \mathcal{L}_\infty$. Therefore, $\exists \zeta_1 \in \mathbb{R}^+$ such that $\mathbf{Y}_{\sigma(t_{l+1}^-)}^T \Theta_{\sigma(t_{l+1}^-)}^* \leq \zeta_1 \ \forall \sigma \in \Omega$ when $\|\mathbf{r}_\sigma\| < \varphi$. Hence, replacing this relation in (32) yields

$$\dot{V}(t) \leq -\kappa V(t) - (\zeta - \kappa)V(t) + \varphi \zeta_1 + \zeta + \zeta_2, \quad t \in (t_l \ t_{l+1}). \quad (32)$$

Note that (32) highlights, for Scenario 2, the exponential decrease of the Lyapunov function in a region around the origin. Further, define the scalar

$$\mathcal{B} \triangleq \frac{\varphi \zeta_1 + \zeta + \zeta_2}{(\zeta - \kappa)}. \quad (33)$$

182 From the two possible scenarios S1 and S2, it can be concluded that $\dot{V}(t) \leq -\kappa V(t)$ when $V(t) \geq \mathcal{B}$ for
183 $t \in (t_l \ t_{l+1})$.

184

185 **Overall behavior of the Lyapunov function:** In light of this, further analysis is needed to observe the
186 overall behaviour of $V(t), t \in (t_l \ t_{l+1})$ for two possible cases:

187 (i) when $V(t) \geq \mathcal{B}$, we have $\dot{V}(t) \leq -\kappa V(t)$ from (29) implying exponential decrease of $V(t)$;

188 (ii) when $V(t) < \mathcal{B}$, $V(t)$ may increase.

189 The analysis of the overall behaviour of $V(t)$ (i.e. the combined behaviour at and in between switching
190 instants) follows similar steps as the analysis of cases (i), (ii) in the proof of Theorem 1 in [31]. Therefore,
191 we do repeat the analysis to avoid repetitions. At the end of such analysis, one obtains that once $V(t)$ enters
192 the interval $[0, \mathcal{B}]$, it cannot exceed the bound $c\mu\mathcal{B}$ any time later with the ADT switching law (14), where
193 $c \triangleq \exp(N_0 \ln \mu)$ is a constant.

Ultimate bound on tracking error: Further, based on this analysis, we have

$$V(t) \leq \max\{cV(t_0), c\mu\mathcal{B}\}, \quad \forall t \geq t_0. \quad (34)$$

Again, the definition of the Lyapunov function (16) yields

$$V(\xi(t), \tilde{\theta}_{ip}(t), \gamma_{ip}(t), t) \geq (1/2)\lambda_{\min}(\mathbf{P}_{\sigma(t)})\|\xi(t)\|^2 \geq (\underline{\zeta}_m/2)\|\xi(t)\|^2, \quad \forall t. \quad (35)$$

Using (34) and (35) we have

$$\|\xi(t)\|^2 \leq (2/\underline{\zeta}_m) \max\{cV(t_0), c\mu\mathcal{B}\}, \quad \forall t \geq t_0. \quad (36)$$

Therefore, using the expressions of μ , \mathcal{B} and c from (14), (33) and (30), an ultimate bound b on the tracking error ξ can be found from (36) as

$$b = \sqrt{\frac{2\bar{\zeta}_M^{(N_0+1)}(\varphi\zeta_1 + \zeta + \zeta_2)}{\underline{\zeta}_m^{(N_0+2)}(\zeta - \kappa)}}. \quad (37)$$

194 Observing the stability arguments, it can be concluded that the closed-loop system is UUB with the control
195 laws (8) and (11) in conjunction with the adaptive law (12) and switching law (14). \square

196 **Remark 4.** The importance of the auxiliary gain $\gamma_{i\bar{p}}$ in system stability can be realized from the following
 197 two observations: first, the term $\hat{\theta}_{i\bar{p}}^2$ on the right hand side of (26) was specifically cancelled by the similar
 198 term on the right side of (25), a consequence of the relations (22)-(24), to arrive at (27). In absence of
 199 $\gamma_{i\bar{p}}$ this would not have been achieved and, system stability could not be ensured. The second observation
 200 concerns the selection of a positive lower bound for $\gamma_{i\bar{p}}$ in (13). Note that the second term on the right
 201 side of (23) comes from the corresponding term of (22), by utilizing the condition $\gamma_{i\bar{p}} \geq \underline{\gamma}_{i\bar{p}}$. This validates
 202 the utility of the selection of a positive lower bound for $\gamma_{i\bar{p}}$ while the lower bounds for the other gains $\hat{\theta}_i$
 203 $i = 0, 1, 2$ are designed as zero.

204 **Remark 5.** The gain (11) reveals that if \bar{E}_σ is taken close to 1, then the gain ρ_σ increases (as $\frac{1}{1-\bar{E}_\sigma}$
 205 increases); higher values of ω in (8b) also increase the effective weight of ρ_σ in $\Delta\tau_\sigma$: these higher gain
 206 conditions lead to faster robust adaptation (via $\Delta\tau_\sigma$) at the cost of higher control input τ_σ (cf. (8a)).
 207 Therefore, these parameters should be tuned according to the trade-off between tracking performance and
 208 control effort depending on application requirements.

209 5. Simulation Results

210 This section studies the effectiveness of the proposed controller using a simplified scenario with pick-
 211 and-place robotic manipulator, often modelled via switched EL dynamics with two subsystems with differ-
 212 ent system parameters (one for the pick phase and one for the place phase) [34]:

$$\mathbf{M}_\sigma(\mathbf{q})\ddot{\mathbf{q}} + \mathbf{C}_\sigma(\mathbf{q}, \dot{\mathbf{q}})\dot{\mathbf{q}} + \mathbf{G}_\sigma(\mathbf{q}) + \mathbf{F}_\sigma(\dot{\mathbf{q}}) + \mathbf{d}_\sigma = \tau_\sigma, \quad (38)$$

$$\begin{aligned} \mathbf{M}_\sigma &= \begin{bmatrix} M_{\sigma 11} & M_{\sigma 12} \\ M_{\sigma 12} & M_{\sigma 22} \end{bmatrix}, \mathbf{q} = \begin{bmatrix} q_l \\ q_u \end{bmatrix}, \\ M_{\sigma 11} &= (m_{\sigma_l} + m_{\sigma_u})l_{\sigma_u}^2 + m_{\sigma_u}l_{\sigma_l}(l_{\sigma_l} + 2l_{\sigma_u}\cos(q_u)), \\ M_{\sigma 12} &= m_{\sigma_u}l_{\sigma_u}(l_{\sigma_u} + l_{\sigma_l}\cos(q_u)), M_{\sigma 22} = m_{\sigma_u}l_{\sigma_u}^2, \\ \mathbf{C}_\sigma &= \begin{bmatrix} -m_{\sigma_u}l_{\sigma_l}l_{\sigma_u}\sin(q_u)\dot{q}_u & -m_{\sigma_u}l_{\sigma_l}l_{\sigma_u}\sin(q_u)(\dot{q}_l + \dot{q}_u) \\ 0 & m_{\sigma_u}l_{\sigma_l}l_{\sigma_u}\sin(q_u)\dot{q}_u \end{bmatrix}, \\ \mathbf{G}_\sigma &= \begin{bmatrix} m_{\sigma_l}l_{\sigma_l}g\cos(q_l) + m_{\sigma_u}g(l_{\sigma_u}\cos(q_l + q_u) + l_{\sigma_l}\cos(q_l)) \\ m_{\sigma_u}gl_{\sigma_u}\cos(q_l + q_u) \end{bmatrix}, \\ \mathbf{F}_\sigma &= \begin{bmatrix} f_{\sigma_{vl}} \frac{\dot{q}_l}{\sqrt{\dot{q}_l^2 + 0.1}} \\ f_{\sigma_{vu}} \frac{\dot{q}_u}{\sqrt{\dot{q}_u^2 + 0.1}} \end{bmatrix}, \mathbf{d}_\sigma = \begin{bmatrix} 0.5 \sin(0.05t) \\ 0.5 \sin(0.05t) \end{bmatrix}, \end{aligned}$$

213 where (m_{p_l}, l_{p_l}, q_l) and (m_{p_u}, l_{p_u}, q_u) denote the mass, length and position of link 1 and 2 respectively for
 214 subsystem p with $p = [1, 2]$. Note that the term \mathbf{F}_σ approximates an unknown static friction. The actual
 215 (and unknown) parametric values of the manipulator subsystems are taken as

- 216 1. $m_{1_l} = m_{1_u} = 2.4\text{kg}$, $l_{1_l} = l_{1_u} = 1\text{m}$, $f_{1_{vl}} = f_{1_{vu}} = 0.6$,
- 217 2. $m_{2_l} = m_{2_u} = 3.6\text{kg}$, $l_{2_l} = l_{2_u} = 1\text{m}$, $f_{2_{vl}} = f_{2_{vu}} = 0.8$,

218 with $g = 9.8\text{m/sec}^2$ for both subsystems. Note that each of the subsystems satisfies Properties 1-2 in As-
 219 sumption 1, whereas the objective is to track a desired trajectory defined as $\{q_l^d, q_u^d\} = \{\sin(0.5t), 0.5 \sin(0.5t)\}\text{rad}$.

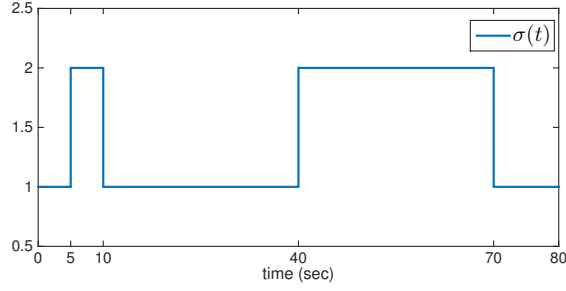


Figure 1: The switching signal.

220 Selection of $\mathbf{K}_{11} = 150\mathbf{I}$, $\mathbf{K}_{21} = 90\mathbf{I}$, $\mathbf{K}_{12} = 200\mathbf{I}$, $\mathbf{K}_{22} = 100\mathbf{I}$, $\mathbf{Q}_1 = \mathbf{Q}_2 = 0.2\mathbf{I}$ yields the ADT $\vartheta^* =$
 221 7.70sec according to (14) when $\kappa = 0.9\zeta$. Therefore, a switching law $\sigma(t)$ is designed as in Fig. 1 (fast
 222 switching is compensated by slower switching).

223 To design $\hat{\mathbf{M}}_p$ in (8a), we select the nominal parameter as $m_{1_l} = m_{1_u} = 2.0\text{kg}$, $l_{1_l} = l_{1_u} = 0.9\text{m}$ and
 224 $m_{2_l} = m_{2_u} = 3.0\text{kg}$, $l_{2_l} = l_{2_u} = 0.9\text{m}$: for such nominal values, Assumption 2 is satisfied with $\bar{E}_1 = \bar{E}_2 = 0.7$.
 225 The terms \mathbf{C}_σ , \mathbf{F}_σ , \mathbf{G}_σ and \mathbf{d}_σ are considered to be completely unknown. Other control design parameters
 226 are selected as $\varepsilon = 0.1$, $\omega = 2$, $\alpha_{i_p} = \beta_{i_{\bar{p}}} = 0.5$, $\bar{v}_{i_{\bar{p}}} = 1$, $v_{i_{\bar{p}}} = 10^{-4}$ with $i = 0, 1, 2$. The initial gain and link
 227 positions are selected as $\hat{\theta}_{0_p}(0) = 1.5 \times 10^{-4}$, $\hat{\theta}_{1_p}(0) = 5 \times 10^{-5}$, $\hat{\theta}_{2_p}(0) = 3 \times 10^{-5}$, $\gamma_{i_{\bar{p}}}(0) = 1.5 \times 10^{-4}$
 228 and $q_l(0) = q_u(0) = 0.5\text{rad}$, respectively.

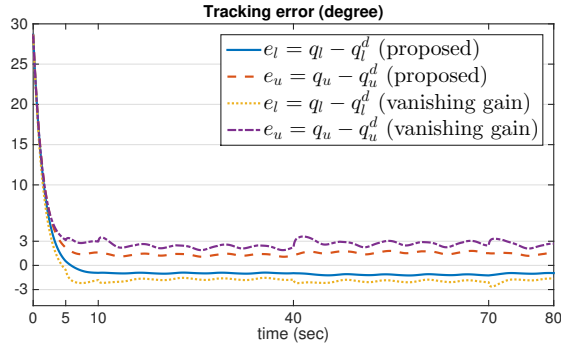


Figure 2: Tracking performance comparison.

To properly judge the performance of the new leakage mechanism against state-of-the-art vanishing gain mechanism, we have compared the proposed controller with the following one, inspired from [26]

$$\rho_\sigma = \frac{1}{1 - \bar{E}_\sigma} \{ \hat{\theta}_{0_\sigma} + \hat{\theta}_{1_\sigma} \|\xi\| + \hat{\theta}_{2_\sigma} \|\xi\|^2 \} \quad (39)$$

$$\dot{\hat{\theta}}_{i_p} = \|\mathbf{r}_p\| \|\xi\|^i - \alpha_{i_p} \hat{\theta}_{i_p}, \quad (40)$$

$$\dot{\hat{\theta}}_{i_{\bar{p}}} = -\alpha_{i_{\bar{p}}} \hat{\theta}_{i_{\bar{p}}}, \quad (41)$$

$$\text{with } \hat{\theta}_{i_p}(t_0), \hat{\theta}_{i_{\bar{p}}}(t_0) > 0, \quad i = 0, 1, 2, \quad (42)$$

229 while (8) remains unchanged. Note that (39)-(42) is a vanishing gain scheme, where the inactive gains $\hat{\theta}_{i_{\bar{p}}}$
 230 decrease exponentially. For parity in comparison, the same control parameters and initial gain conditions

231 are selected for both controllers with $\alpha_{ip} = 0.5$.

232 The tracking performance of the proposed controller is depicted in Fig. 2, in comparison with the
 233 vanishing gain scheme. It is clear that, beside having worse steady-state performance, the vanishing gain
 234 scheme has worse transient behaviour at each switching instants. This can be clearly explained by the
 235 evolutions of control gains for these two control schemes, as shown in Figs. 3-5. For all these figures it is
 236 worth mentioning that $\hat{\theta}_{0\sigma}$, $\hat{\theta}_{1\sigma}$, $\hat{\theta}_{2\sigma}$ have different orders of magnitude but similar trends ($\hat{\theta}_{0\sigma}$ is the largest
 237 gain and one should zoom in to better see the trends of $\hat{\theta}_{1\sigma}$ and $\hat{\theta}_{2\sigma}$).

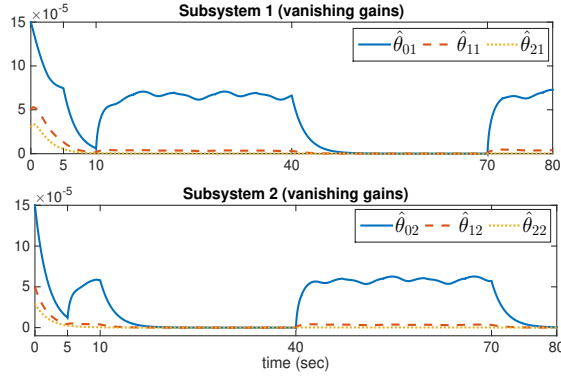


Figure 3: Evolution of gains under 'vanishing gain' scheme.

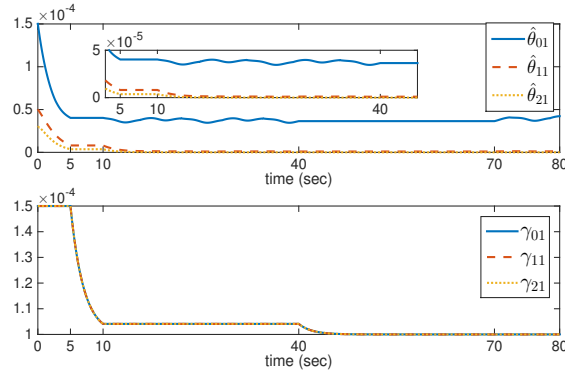


Figure 4: Gains for subsystem 1 with the proposed controller.

238 Fig. 3 clearly shows the state-of-the-art vanishing gain mechanism during inactive times: for example,
 239 during $t = [5 - 10)$ sec and $t = [40 - 70)$ sec when subsystem 1 was switched-off, $\hat{\theta}_{01}$ kept decreasing (i.e.,
 240 kept vanishing); as a result, when it was again switched on at $t = 10$ sec and $t = 70$ sec, it had to adapt itself
 241 again, causing a transient at every switch-on instances. Similar situation can be noticed for $\hat{\theta}_{02}$ as well.
 242 Control gains dropping to zero essentially means no control, which is in general not desirable. Whereas,
 243 for the proposed scheme, Figs. 4 and 5 highlight that the vanishing trend has been removed. The different
 244 orders of magnitude also show that the upper bound structure in (5) is adaptively shaped in such a way to
 245 give more weight to low power coefficients (i.e. $\hat{\theta}_{0\sigma}$). To further demonstrate robustness against noise, the
 246 tracking performance of the proposed controller is depicted in Fig. 6 when a Gaussian noise of variance
 247 0.001 is inserted in the feedback path for both \mathbf{q} and $\dot{\mathbf{q}}$.

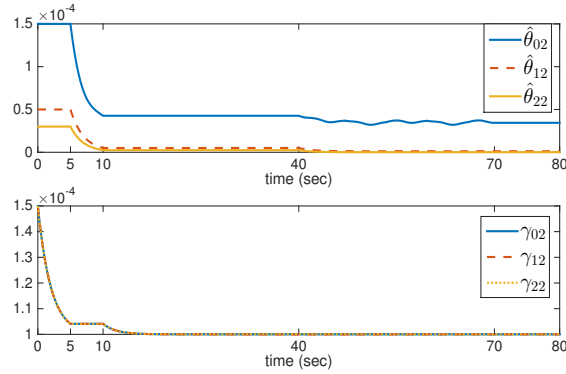


Figure 5: Gains for subsystem 2 with the proposed controller.

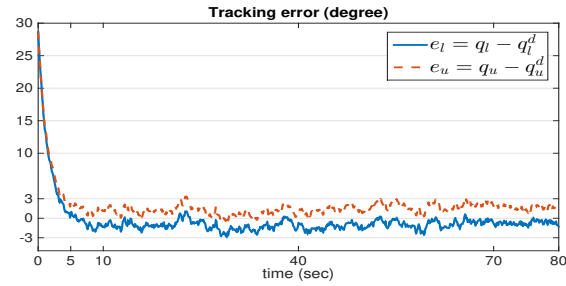


Figure 6: Tracking performance of the proposed controller with noise.

248 6. Conclusions

249 A new concept of robust adaptation with leakage mechanism for uncertain switched EL systems was
 250 presented in this paper. The issue of vanishing gains of inactive subsystems was completely eliminated
 251 by virtue of properly designed auxiliary gains. At the same time, unmodelled dynamics and uncertainties
 252 with no a priori bounds could be handled by a quadratic state-dependent upper bound structure that reduces
 253 conservativeness as compared to state-of-the-art structures. Bounded stability analysis and simulations with
 254 a pick-and-place robotic manipulator example have been provided.

255 Relevant future work would be to consider state-dependent switching or impulsive behaviour, or larger
 256 classes of nonlinear systems such as underactuated or nonholonomic systems [35, 36].

257 References

- 258 [1] Liberzon D. Switching in systems and control. Springer Science & Business Media; 2003.
 259 [2] Hespanha JP, Morse AS. Stability of switched systems with average dwell-time. In: Proceedings of the 38th IEEE Conference
 260 on Decision and Control. 1999, p. 2655–60.
 261 [3] Zhang L, Gao H. Asynchronously switched control of switched linear systems with average dwell time. Automatica
 262 2010;46(5):953–8.
 263 [4] Zhao X, Zhang L, Shi P, Liu M. Stability and stabilization of switched linear systems with mode-dependent average dwell
 264 time. IEEE Transactions on Automatic Control 2012;57(7):1809–15.
 265 [5] Allerhand LI, Shaked U. Robust stability and stabilization of linear switched systems with dwell time. IEEE Transactions on
 266 Automatic Control 2011;56(2):381–6.
 267 [6] Battistelli G, Mari D, Selvi D, Tesi A, Tesi P. Adaptive disturbance attenuation via logic-based switching. Systems & Control
 268 Letters 2014;73:48 – 57.

- 269 [7] Zhao X, Zheng X, Niu B, Liu L. Adaptive tracking control for a class of uncertain switched nonlinear systems. *Automatica* 2015;52:185–91.
- 270
- 271 [8] Wu JL. Stabilizing controllers design for switched nonlinear systems in strict-feedback form. *Automatica* 2009;45(4):1092–6.
- 272 [9] Xudong Y. Nonlinear adaptive control by switching linear controllers. *Systems & Control Letters* 2012;61(4):617–21.
- 273 [10] Basu Roy S, Bhasin S, Kar IN. Robust gradient-based adaptive control of nonlinearly parametrized plants. *IEEE Control*
- 274 *Systems Letters* 2017;1(2):352–7.
- 275 [11] Chen W, Wen C, Wu J. Global exponential/finite-time stability of nonlinear adaptive switching systems with applications in
- 276 controlling systems with unknown control direction. *IEEE Transactions on Automatic Control* 2018;63(8):2738–44.
- 277 [12] Bikas LN, Rovithakis GA. Combining prescribed tracking performance and controller simplicity for a class of uncertain
- 278 mimo nonlinear systems with input quantization. *IEEE Transactions on Automatic Control* 2019;64(3):1228–35.
- 279 [13] Aghababa MP. Finite time control of a class of nonlinear switched systems in spite of unknown parameters and input
- 280 saturation. *Nonlinear Analysis: Hybrid Systems* 2019;31:220–32.
- 281 [14] Sang Q, Tao G. Adaptive control of piecewise linear systems: the state tracking case. *IEEE Transactions on Automatic*
- 282 *Control* 2012;57(2):522–8.
- 283 [15] di Bernardo M, Montanaro U, Santini S. Hybrid model reference adaptive control of piecewise affine systems. *IEEE*
- 284 *Transactions on Automatic Control* 2013;58(2):304–16.
- 285 [16] di Bernardo M, Montanaro U, Ortega R, Santini S. Extended hybrid model reference adaptive control of piecewise affine
- 286 systems. *Nonlinear Analysis: Hybrid Systems* 2016;21:11–21.
- 287 [17] Yuan S, De Schutter B, Baldi S. Adaptive asymptotic tracking control of uncertain time-driven switched linear systems. *IEEE*
- 288 *Transactions on Automatic Control* 2017;62(11):5802–7.
- 289 [18] Chiang ML, Fu LC. Adaptive stabilization of a class of uncertain switched nonlinear systems with backstepping control.
- 290 *Automatica* 2014;50(8):2128–35.
- 291 [19] Long L, Wang Z, Zhao J. Switched adaptive control of switched nonlinearly parameterized systems with unstable subsystems.
- 292 *Automatica* 2015;54:217–28.
- 293 [20] Wang CY, Jiao XH. Adaptive control under arbitrary switching for a class of switched nonlinear systems with nonlinear
- 294 parameterisation. *International Journal of Control* 2015;88(10):2044–54.
- 295 [21] Hosseinzadeh M, Yazdanpanah MJ. Performance enhanced model reference adaptive control through switching non-quadratic
- 296 lyapunov functions. *Systems & Control Letters* 2015;76:47–55.
- 297 [22] Noghreian E, Koofgar HR. Adaptive output feedback tracking control for a class of uncertain switched nonlinear systems
- 298 under arbitrary switching. *International Journal of Systems Science* 2018;49(3):486–95.
- 299 [23] Lou ZE, Zhao J. Immersion-and invariance-based adaptive stabilization of switched nonlinear systems. *International Journal*
- 300 *of Robust and Nonlinear Control* 2018;28(1):197–212.
- 301 [24] Lai G, Liu Z, Zhang Y, Chen CP, Xie S. Adaptive backstepping-based tracking control of a class of uncertain switched
- 302 nonlinear systems. *Automatica* 2018;91:301–10.
- 303 [25] Ioannou PA, Sun J. Robust adaptive control. PTR Prentice-Hall Upper Saddle River, NJ; 1996.
- 304 [26] Yuan S, De Schutter B, Baldi S. Robust adaptive tracking control of uncertain slowly switched linear systems. *Nonlinear*
- 305 *Analysis: Hybrid Systems* 2018;27:1–12.
- 306 [27] Roy S, Baldi S. A simultaneous adaptation law for a class of nonlinearly parametrized switched systems. *IEEE Control*
- 307 *Systems Letters* 2019;3(3):487–92.
- 308 [28] Zhai D, Xi C, An L, Dong J, Zhang Q. Prescribed performance switched adaptive dynamic surface control of switched nonlin-
- 309 ear systems with average dwell time. *IEEE Transactions on Systems, Man, and Cybernetics: Systems* 2017;47(7):1257–69.
- 310 [29] Lin W, Qian C. Adaptive control of nonlinearly parameterized systems: a nonsmooth feedback framework. *IEEE Transac-*
- 311 *tions on Automatic control* 2002;47(5):757–74.
- 312 [30] Spong MW, Hutchinson S, Vidyasagar M. Robot dynamics and control. John Wiley & Sons; 2008.
- 313 [31] Roy S, Baldi S. On reduced-complexity robust adaptive control of switched euler–lagrange systems. *Nonlinear Analysis:*
- 314 *Hybrid Systems* 2019;34:226–37.
- 315 [32] Roy S, Roy SB, Lee J, Baldi S. Overcoming the underestimation and overestimation problems in adaptive sliding mode
- 316 control. *IEEE/ASME Transactions on Mechatronics* 2019;24(5):2031–9.
- 317 [33] Shtessel Y, Taleb M, Plestan F. A novel adaptive-gain supertwisting sliding mode controller: Methodology and application.
- 318 *Automatica* 2012;48(5):759–69.
- 319 [34] Wang X, Zhao J. Autonomous switched control of load shifting robot manipulators. *IEEE Transactions on Industrial Elec-*
- 320 *tronics* 2017;64(9):7161–70.
- 321 [35] Ashrafiuon H, Nersesov S, Clayton G. Trajectory tracking control of planar underactuated vehicles. *IEEE transactions on*
- 322 *automatic control* 2016;62(4):1959–65.
- 323 [36] Roy S, Baldi S. Towards structure-independent stabilization for uncertain underactuated euler–lagrange systems. *Automatica*
- 324 2020;113:108775.